Ultracold collisions of Cs atoms in excited Zeeman and hyperfine states

Matthew D. Frye ◉, B. C. Yang, and Jeremy M. Hutson*

Joint Quantum Centre (JQC) Durham-Newcastle, Department of Chemistry, Durham University,
South Road, Durham DH1 3LE, United Kingdom

We investigate Cs + Cs scattering in excited Zeeman and hyperfine states. We calculate the real and imaginary parts of the s-wave scattering length; the imaginary part directly provides the rate coefficient for two-body inelastic loss, while the real part allows us to identify regions of magnetic field where three-body recombination will be slow. We identify field regions where Cs in its $(f, m_f) = (3, +2)$ and $(3, +1)$ states may be stable enough to allow Bose-Einstein condensation, and additional regions for these and the $(3, 0)$ and $(3, -3)$ states where high-density clouds should be long-lived.

I. INTRODUCTION

The ability to cool atoms to ultracold temperatures has opened up a huge field of physics over the past three decades. A key feature of ultracold atoms is the ability to control the interatomic interactions by varying the scattering length a. This is most commonly done using a zero-energy Feshbach resonance, where a bound state crosses a threshold as a function of magnetic field B [1]. In the absence of inelastic scattering, there is a resonant pole in $a(B)$ [2] that allows essentially any scattering length to be obtained with sufficiently good field control.

The scattering length shows very different behavior for different atomic species. For the alkali metals, which are particularly commonly used, every stable isotope exhibits Feshbach resonances at experimentally accessible magnetic fields. However, widths and background scattering lengths vary enormously, making each isotope suitable for a different range of experiments [1]. Indeed, even different Zeeman and hyperfine states of the same isotope have different properties and may find different applications.

A pair of alkali-metal atoms in their ^{2}S electronic ground state may interact on singlet ($^1\Sigma_g^+$) or triplet ($^3\Sigma_u^+$) potential curves. Each of these is characterized by a single (field-independent) scattering length, a_s and a_t, respectively. Different Zeeman and hyperfine states experience different combinations of the singlet and triplet interactions and have Feshbach resonances at different fields. In general terms, Feshbach resonances due to s-wave states crossing the threshold are narrow if $a_s \approx a_t$ but may be broad otherwise. The alkali-metal atoms with the broadest resonances and therefore the most precisely tunable scattering lengths are ^{6}Li [3–5], ^{39}K [6], and ^{133}Cs [7–11].

Cs has a very large positive triplet scattering length $a_t = 2858(19)a_0$ and a moderate positive singlet scattering length $a_s = 286.5(10)a_0$ [11]. For its lowest Zeeman state, $(f, m_f) = (3, +3)$, there are many resonances, some of which are very broad. The broad resonances provide excellent control over the scattering length, making Cs an attractive atom for studies of strongly interacting Bose gases [12] and Efimov physics [13–15]. Mixtures of Cs with other species are also of interest, particularly for studying systems with large mass imbalances [16–20] and for heteronuclear molecule formation [21–24]. However, the intraspecies scattering length for Cs $(3, +3)$ is very large at fields away from resonance, causing fast three-body recombination [25] at most magnetic fields and making it challenging to work with high Cs densities. In particular, it has been possible to cool Cs $(3, +3)$ close to degeneracy only at a few specific magnetic fields; it is usually done at the Efimov minimum in three-body recombination near 21 G [13], but it is also possible around 558.7 and 894 G [11].

The dependence of the scattering length on magnetic field is well known for Cs $(3, +3)$. Feshbach resonance positions and near-threshold bound-state energies at fields up to 1000 G have been fitted to obtain precise singlet and triplet potential curves, and the calculated scattering length has been tabulated for magnetic fields up to 1200 G [11]. In addition, a considerable amount of early work used Cs in its magnetically trappable states $(3, -3)$ and $(4, +4)$ [7,26–30], while Chin *et al.* [8,10] observed Feshbach resonances in a variety of states and in mixtures at magnetic fields up to 230 G. These were interpreted to obtain early interaction potentials [9,10]. However, relatively little has been done on the excited states since Bose-Einstein condensation was achieved in the $(3, +3)$ state [31], and the interaction potentials of Refs. [9] and [10] do not predict resonance positions accurately at higher fields [11]. There is a clear need for a thorough investigation of the collisional properties of Cs in excited Zeeman and hyperfine states, using the most recent interaction potential [11]. Excited Cs atoms may provide new species with new Feshbach resonances and additional regions of stability. This may be particularly valuable for mixture experiments in which interspecies resonances appear at specific fields [21,22,32], or where the second atom itself imposes limitations on the fields that can be used [22,33].

*j.m.hutson@durham.ac.uk

II. THEORY

We perform coupled-channel scattering calculations on the interaction potential of Berninger *et al.* [11]. The methods used are similar to those in Ref. [11], so only a brief outline is given here. The Hamiltonian for the interacting pair is

$$\hat{H} = \frac{\hbar^2}{2\mu}\left[-\frac{1}{R}\frac{d^2}{dR^2}R + \frac{\hat{L}^2}{R^2}\right] + \hat{H}_A + \hat{H}_B + \hat{V}(R), \quad (1)$$

where R is the internuclear distance, μ is the reduced mass, and $\hbar$ is the reduced Planck constant. $\hat{L}$ is the two-atom rotational angular momentum operator. The single-atom Hamiltonians $\hat{H}_i$ contain the hyperfine couplings and the Zeeman interaction with the magnetic field. The interaction operator $\hat{V}(R)$ contains the two isotropic Born-Oppenheimer potentials, for the $X\,^1\Sigma_g^+$ singlet and $a\,^3\Sigma_u^+$ triplet states, and anisotropic spin-dependent couplings that arise from dipole-dipole and second-order spin-orbit coupling.

Scattering calculations are carried out using the MOLSCAT package [34]. The scattering wave function is expanded in a fully uncoupled basis set that contains all allowed spin functions, limited by $L_{max} = 4$. The collision energy is $E = 1$ nK $\times k_B$. Solutions are propagated from $R_{min} = 6a_0$ to $R_{mid} = 20a_0$ using the diabatic modified log-derivative propagator (LDMD) of Manolopoulos [35] with a step size of $0.002a_0$, and from R_{mid} to $R_{max} = 10\,000a_0$ using the log-derivative Airy propagator of Alexander and Manolopoulos [36] with a variable step size. The Airy propagator can take large steps when the interaction potential is weak and slowly varying, so it is highly efficient in the long-range region outside R_{mid}. However, the LDMD propagator gives better step-size convergence in the well region, where the interaction potential is strong. The log-derivative matrix is transformed into the asymptotic basis set at R_{max} and matched to S-matrix boundary conditions to obtain the scattering matrix **S**.

For collisions of Cs in its lowest state $(3, +3)$, only elastic collisions are possible. For collisions of atoms in excited states, however, inelastic scattering may occur. Inelastic collisions that produce atoms in lower-lying states release kinetic energy and usually produce heating or trap loss. The inelastic collisions are of two types: spin exchange and spin relaxation. Collisions that conserve $M_F = m_{f,A} + m_{f,B}$ are termed spin-exchange collisions, while those that do not conserve M_F are termed spin-relaxation collisions. Spin-exchange collisions are driven mostly by the difference between the singlet and triplet interactions, whereas spin-relaxation collisions are driven by the much weaker anisotropic couplings.

Spin-exchange collisions are generally fast when they are energetically allowed. However, for pairs of alkali-metal atoms in the lower hyperfine state ($f = 3$ for Cs), they are endoergic. The incoming and outgoing channels have the same linear Zeeman energy, but they are separated by terms that are quadratic in B at low field. At 10 G, spin-exchange collisions are allowed for collision energies above 130 nK $\times k_B$. Below this threshold, only spin relaxation can produce inelasticity.

Both elastic and inelastic collisions are conveniently characterized in terms of the energy-dependent s-wave scattering length [37],

$$a(k) = \frac{1}{ik}\left(\frac{1 - S_{00}(k)}{1 + S_{00}(k)}\right), \quad (2)$$

where $k = \sqrt{2\mu E}/\hbar$ is the wave vector and S_{00} is the diagonal S-matrix element in the incoming channel. When there is only one open channel, only elastic scattering is possible and $a(k)$ is real. When inelastic scattering is possible, however, $a(k)$ is complex, $a(k) = \alpha(k) - i\beta(k)$. The dominant ($s$-wave) contribution to the rate coefficient for two-body loss is [37]

$$k_2 = \frac{4\pi\hbar\beta}{\mu(1 + k^2|a|^2 + 2k\beta)}. \quad (3)$$

This expression for k_2 can contain small contributions from collisions that are incoming in the s-wave channel and change L without changing the internal state of the atoms, but these vanish as $E \to 0$ and are negligible at the collision energies considered here. When the k-dependence of the denominator of Eq. (3) can be neglected, $\beta = 1a_0$ corresponds to $k_2 = 1.3 \times 10^{-12}$ cm^3 s^{-1}.

Both the scattering length and the loss rate are independent of energy in the limit $E \to 0$. Deviations from this reach around 2% at $E = 100$ nK $\times k_B$, but they are negligible at the energy of our calculations. Inelastic rates from s-wave collisions generally decrease with energy except as discussed below for spin-exchange collisions. The height of the d-wave centrifugal barrier is 180 μK $\times k_B$, and d-wave contributions to k_2 are generally small at collision energies below 50 μK $\times k_B$, except near narrow resonances.

In the presence of inelastic scattering, the real and imaginary parts of the scattering length show an oscillation across a resonance rather than a pole. The form of the oscillation was discussed in Ref. [37]. If the background inelastic scattering is negligible, $\alpha(B)$ shows an oscillation of amplitude $\pm a_{res}/2$ and β shows a peak of magnitude a_{res}. If the background inelastic scattering is significant, the oscillation is more complicated. For the states of Cs considered here, α_{bg} is typically several hundred a_0 or more, while β_{bg} is often in the range $0 < \beta < 10a_0$. It is therefore common for decayed resonances to be visible in plots of k_2 (obtained from β) but not in the corresponding plots of α.

Losses may occur due to three-body recombination as well as two-body inelastic processes. Three-body recombination rates depend strongly on the scattering length, and they are typically proportional to a^4 when a is large [25]. For Cs in its $(3, +3)$ state, such losses are generally fast except in limited ranges of magnetic field near broad resonances, where either the scattering length is near a zero-crossing or three-body losses are suppressed by an Efimov minimum [13]. Evaporative cooling is most efficient near an Efimov minimum, since it requires elastic collisions and the elastic cross section vanishes at a zero-crossing. For broad resonances in Cs, Efimov minima typically occur when $a \sim 200a_0$ to $300a_0$ [11].

III. RESULTS

We have carried out coupled-channel scattering calculations for pairs of Cs atoms initially in the same state (f, m_f) for all $f = 3$ and 4 states. The calculations are carried out at fields from 0 to 2000 G in steps of 0.1 G. We calculate the real and imaginary parts of the scattering length, $\alpha(B)$ and $\beta(B)$, and express the latter as the two-body inelastic rate coefficient $k_2(B)$. Figures 1 and 2 show the results for $f = 3$, $m_f \geqslant 0$ and $m_f < 0$, respectively. The gray bars show where $-200a_0 < \alpha < 500a_0$ to indicate regions where the three-body
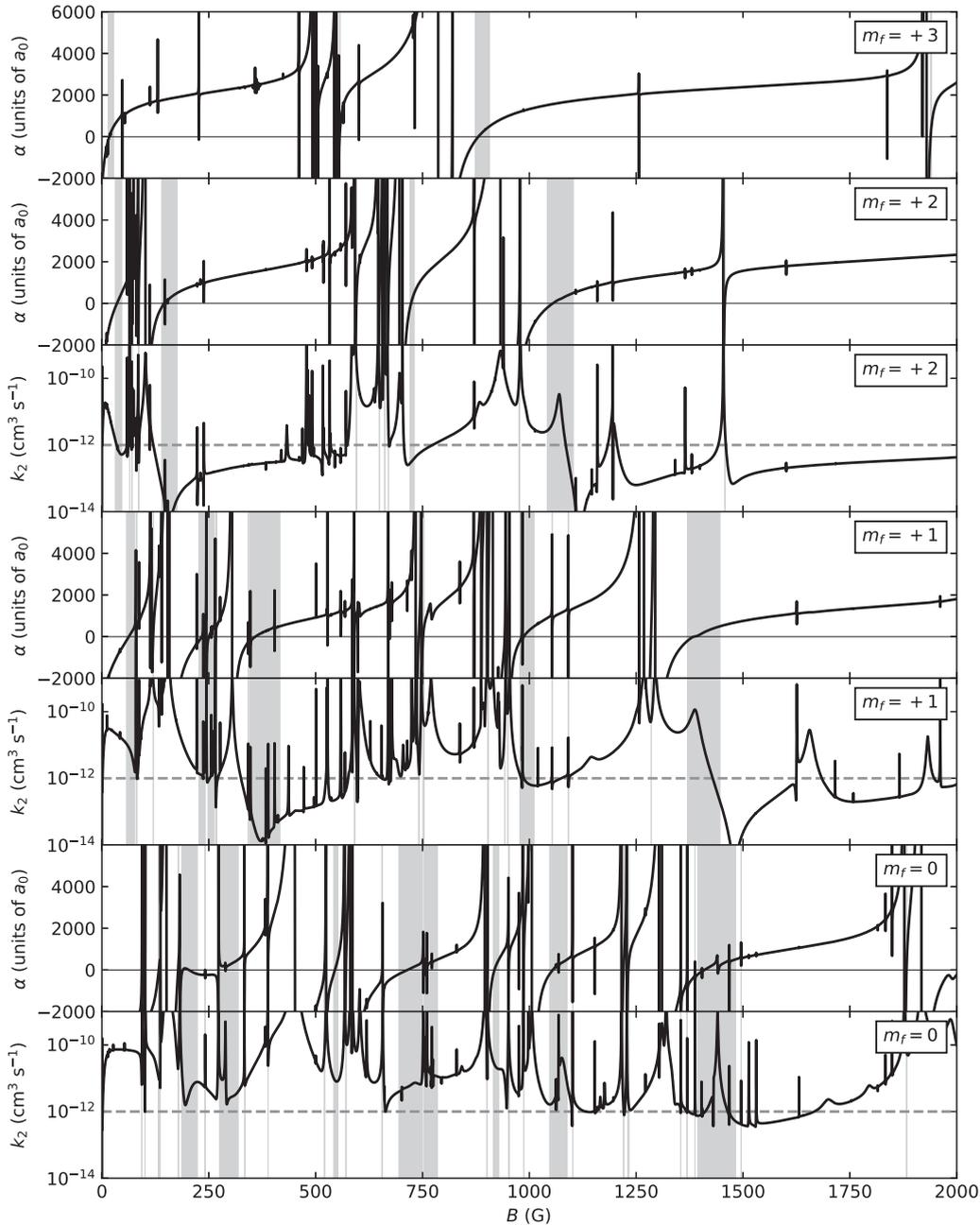
FIG. 1. Real part of the scattering length α and inelastic loss rate coefficient k_2 for collisions of pairs of Cs atoms with $f = 3$ and the same m_f for $m_f \geqslant 0$. Shaded regions correspond to fields where $-200a_0 < \alpha < 500a_0$. Calculations are performed on a 0.1 G grid, so narrow resonances are not always visible.

recombination rate is expected to be moderate. The bars serve to guide the eye in reading the corresponding values of k_2.

Before Bose-Einstein condensation was achieved for Cs $(3, +3)$ [31], degeneracy was approached but not achieved for Cs $(3, -3)$. Cooling of $(3, -3)$ was limited by two-body inelastic collisions with $k_2 \approx 2 \times 10^{-12}$ cm^3 s^{-1} at 139 G [30]. We therefore estimate that a rate coefficient higher than about 10^{-12} cm^3 s^{-1} is sufficient to prevent cooling to degeneracy in other states. This value is indicated by dashed horizontal lines in Figs. 1 and 2. It may be noted that we calculate the scattering length for the $(3, -3)$ state at 139 G to be $3200a_0$; this is sufficient to cause substantial three-body losses, which limited the Cs density in Ref. [30].

The scattering length for $m_f = +3$ is known from previous work [11] and will not be discussed in detail here. The regions of moderate scattering length around 21 and 894 G, where cooling is usually performed, are clearly visible; the region near 558.7 G is too narrow to be clearly seen with our scale/grid.

For $m_f = +2$, the behavior of α is broadly similar to that for $m_f = +3$. There are a few very broad resonances and a large number of narrower resonances. Inelastic loss is now possible, and every resonance also creates a corresponding peak in k_2. Many of these peaks are asymmetric and have a dip in loss on one side that arises from interference between background inelastic scattering and inelastic scattering
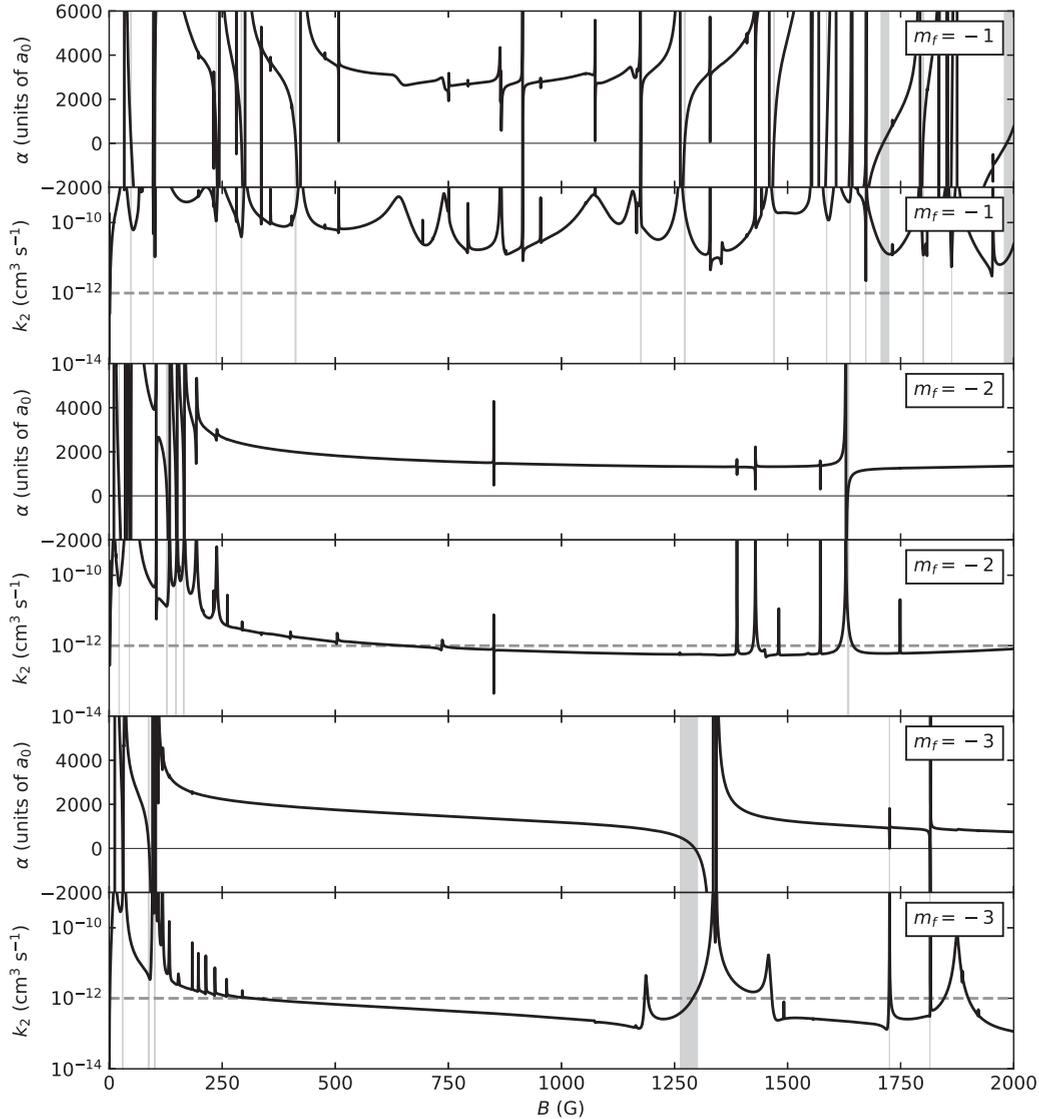
FIG. 2. Real part of the scattering length α and inelastic loss rate coefficient k_2 for collisions of pairs of Cs atoms with $f = 3$ and the same m_f for $m_f < 0$. Shaded regions correspond to fields where $-200a_0 < \alpha < 500a_0$. Calculations are performed on a 0.1 G grid, so narrow resonances are not always visible.

mediated by the resonance [37,38]. If there is a single dominant loss channel, the interference may be almost complete, and k_2 then drops close to zero. However, additional loss channels result in incomplete cancellation and shallower minima. For the broad resonances, these dips can be quite wide and tend to coincide with the regions of moderate scattering length. This results in several ranges where both α and k_2 are small enough to allow experiments with high densities of Cs. The region around 150 G associated with the broad resonance at 100 G appears particularly promising. At 150 G, spin-exchange collisions are allowed at collision energies above $25\,\mu\text{K} \times k_\text{B}$. However, such collisions actually *reduce* the kinetic energy; the $(3, +3)$ and $(3, +1)$ atoms produced will remain confined in an optical trap, and can return to the original state in further collisions. The region below 1100 G, associated with broad resonance near 930 G, is affected by a narrower resonance that is strongly decayed, with $a_\text{res} = 25a_0$, and is thus visible only in the inelastic rate. Because of this,

Cs $(3, +2)$ is likely to exhibit slow two-body loss only at the upper end of this second shaded region, and the low values of k_2 must be balanced against three-body recombination arising from the increasing value of α.

Similar effects are seen for $m_f = +1$. The shaded region between 350 and 400 G is generally favorable, though it contains a number of narrow resonances that will produce loss. The shaded region from 1370 to 1450 G is affected by a narrow resonance that enhances two-body loss at the lower end of the range, so that Cs $(3, +1)$ will probably exhibit slow two-body loss only at the upper end of this range.

The loss rates for $m_f = 0$ and -1 show weaker resonant structure with shallower troughs. Many of the resonances also appear as oscillations in α rather than poles. This is due to the increased number of loss channels. There are few regions with low two-body loss rates, and these do not coincide with moderate α except for a small region near 1500 G for $m_f = 0$.
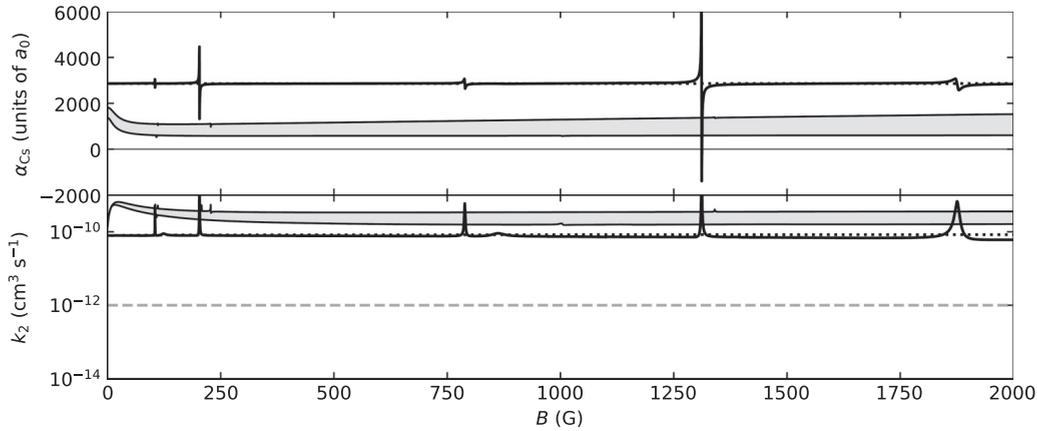
FIG. 3. Real part of the scattering length α and inelastic loss rate coefficient k_2 for collisions of pairs of Cs atoms with $f = 4$ and the same m_f. The solid black line shows $m_f = -4$ while the dotted black line shows $m_f = +4$, which is almost identical except near resonances. The shaded bands show the ranges covered by $-3 \leqslant m_f \leqslant +3$. Calculations are performed on a 0.1 G grid, so narrow resonances are not resolved.

There are significantly fewer resonances visible for $m_f = -2$ and -3 than for the lower states. This is largely because there are fewer closed channels close in energy to support resonant states. α therefore remains large across the whole range for $m_f = -2$. The only broad resonance is at 1340 G for $m_f = -3$ and results in a region of moderate scattering length around 1300 G. The inelastic rate coefficient in this region is about 10^{-12} cm^3 s^{-1}, so reasonably high-density clouds of Cs $(3, -3)$ might be stable.

Figure 3 shows the results for all $f = 4$ states. Both k_2 and α are large over the entire range for all states. The lowest Zeeman state, $m_f = -4$, exhibits the most structure, but there are only a few resonances, which are narrow and significantly decayed. The remaining states have little variation or structure because there are few closed channels at higher energies to support resonant states, and the few resonances that do exist are strongly decayed and thus barely visible on this scale.

IV. CONCLUSIONS

We have carried out coupled-channel calculations on collisions of ultracold Cs in excited Zeeman and hyperfine states in order to identify regions of magnetic field where high-density atomic clouds might be cooled to degeneracy or close to it. We have calculated the real and imaginary parts of the scattering length at magnetic fields up to 2000 G for pairs of atoms in each Zeeman and hyperfine state. The imaginary part of the scattering length gives the rate coefficient for two-body inelastic loss, while the real part allows us to identify regions in which three-body recombination will be relatively slow.

For Cs in its $(f, m_f) = (3, +2)$ and $(3, +1)$ excited states, there are regions where the two-body loss coefficient is very low, $k_2 \lesssim 10^{-14}$ cm^3 s^{-1}, and three-body loss is likely to be suppressed by Efimov effects. These regions are very promising for creating high-density clouds and possibly forming Bose-Einstein condensates. Cs $(3,0)$ is less favorable, as the two-body loss coefficient seldom drops below 10^{-12} cm^3 s^{-1}, but may nevertheless offer possibilities. Cs $(3, -1)$ has even faster two-body losses. Cs $(3, -2)$ has large regions where the two-body loss coefficient is slightly below 10^{-12} cm^3 s^{-1}, but the scattering length is large and there are no broad Feshbach resonances in these regions to moderate three-body losses. $(3, -3)$ has a similar two-body loss coefficient, but in this case there is a broad Feshbach resonance that may produce low three-body losses in a limited region around 1300 G. All the Cs $f = 4$ states experience fast two-body losses across the entire range of fields. There are no substantial regions of magnetic field where two different states of Cs are predicted to have simultaneously low loss rates.

The calculations presented here pave the way to producing high-density clouds of Cs in excited Zeeman states with $f = 3$. These species can be used for the study of ultracold gases, with particular importance in studying atomic mixtures and in heteronuclear molecule formation.

The data presented in this work are available from Durham University [39].

[1] C. Chin, R. Grimm, P. S. Julienne, and E. Tiesinga, Rev. Mod. Phys. **82**, 1225 (2010).

[2] A. J. Moerdijk, B. J. Verhaar, and A. Axelsson, Phys. Rev. A **51**, 4852 (1995).

[3] M. Houbiers, H. T. C. Stoof, W. I. McAlexander, and R. G. Hulet, Phys. Rev. A **57**, R1497(R) (1998).

[4] S. Jochim, M. Bartenstein, G. Hendl, J. Hecker Denschlag, R. Grimm, A. Mosk, and M. Weidemüller, Phys. Rev. Lett. **89**, 273202 (2002).

[5] P. S. Julienne and J. M. Hutson, Phys. Rev. A **89**, 052715 (2014).

[6] C. D'Errico, M. Zaccanti, M. Fattori, G. Roati, M. Inguscio, G. Modugno, and A. Simoni, New J. Phys. **9**, 223 (2007).

[7] V. Vuletić, A. J. Kerman, C. Chin, and S. Chu, Phys. Rev. Lett. **82**, 1406 (1999).

[8] C. Chin, V. Vuletić, A. J. Kerman, and S. Chu, Phys. Rev. Lett. **85**, 2717 (2000).

[9] P. J. Leo, C. J. Williams, and P. S. Julienne, Phys. Rev. Lett. **85**, 2721 (2000).

[10] C. Chin, V. Vuletić, A. J. Kerman, S. Chu, E. Tiesinga, P. J. Leo, and C. J. Williams, Phys. Rev. A **70**, 032701 (2004).

[11] M. Berninger, A. Zenesini, B. Huang, W. Harm, H.-C. Nägerl, F. Ferlaino, R. Grimm, P. S. Julienne, and J. M. Hutson, Phys. Rev. A **87**, 032517 (2013).

[12] F. Chevy and C. Salomon, J. Phys. B **49**, 192001 (2016).

[13] T. Kraemer, M. Mark, P. Waldburger, J. G. Danzl, C. Chin, B. Engeser, A. D. Lange, K. Pilch, A. Jaakkola, H. C. Nägerl, and R. Grimm, Nature (London) **440**, 315 (2006).

[14] M. Berninger, A. Zenesini, B. Huang, W. Harm, H.-C. Nägerl, F. Ferlaino, R. Grimm, P. S. Julienne, and J. M. Hutson, Phys. Rev. Lett. **107**, 120401 (2011).

[15] B. Huang, L. A. Sidorenkov, R. Grimm, and J. M. Hutson, Phys. Rev. Lett. **112**, 190401 (2014).

[16] E. Fratini and P. Pieri, Phys. Rev. A **85**, 063618 (2012).

[17] S.-K. Tung, K. Jimenez-Garcia, J. Johansen, C. V. Parker, and C. Chin, Phys. Rev. Lett. **113**, 240402 (2014).

[18] S. Gopalakrishnan, C. V. Parker, and E. Demler, Phys. Rev. Lett. **114**, 045301 (2015).

[19] L. A. Pena Ardila and S. Giorgini, Phys. Rev. A **94**, 063640 (2016).

[20] B. DeSalvo, K. Patel, G. Cai, and C. Chin, Nature (London) **568**, 61 (2019).

[21] D. A. Brue and J. M. Hutson, Phys. Rev. A **87**, 052709 (2013).

[22] H. J. Patel, C. L. Blackley, S. L. Cornish, and J. M. Hutson, Phys. Rev. A **90**, 032716 (2014).

[23] P. K. Molony, P. D. Gregory, Z. Ji, B. Lu, M. P. Köppinger, C. R. Le Sueur, C. L. Blackley, J. M. Hutson, and S. L. Cornish, Phys. Rev. Lett. **113**, 255301 (2014).

[24] T. Takekoshi, L. Reichsöllner, A. Schindewolf, J. M. Hutson, C. R. Le Sueur, O. Dulieu, F. Ferlaino, R. Grimm, and H.-C. Nägerl, Phys. Rev. Lett. **113**, 205301 (2014).

[25] B. D. Esry, C. H. Greene, and J. P. Burke, Phys. Rev. Lett. **83**, 1751 (1999).

[26] M. Arndt, M. Ben Dahan, D. Guéry-Odelin, M. W. Reynolds, and J. Dalibard, Phys. Rev. Lett. **79**, 625 (1997).

[27] D. Guéry-Odelin, J. Söding, P. Desbiolles, and J. Dalibard, Europhys. Lett. **44**, 25 (1998).

[28] J. Söding, D. Guéry-Odelin, P. Desbiolles, G. Ferrari, and J. Dalibard, Phys. Rev. Lett. **80**, 1869 (1998).

[29] S. A. Hopkins, S. Webster, J. Arlt, P. Bance, S. Cornish, O. Maragò, and C. J. Foot, Phys. Rev. A **61**, 032707 (2000).

[30] A. M. Thomas, S. Hopkins, S. L. Cornish, and C. J. Foot, J. Opt. B **5**, S107 (2003).

[31] T. Weber, J. Herbig, M. Mark, H.-C. Nägerl, and R. Grimm, Science **299**, 232 (2003).

[32] B. C. Yang, M. D. Frye, A. Guttridge, J. Aldegunde, P. S. Żuchowski, S. L. Cornish, and J. M. Hutson, arXiv:1905.11977.

[33] H.-W. Cho, D. J. McCarron, M. P. Köppinger, D. L. Jenkin, K. L. Butler, P. S. Julienne, C. L. Blackley, C. R. Le Sueur, J. M. Hutson, and S. L. Cornish, Phys. Rev. A **87**, 010703(R) (2013).

[34] J. M. Hutson and C. R. Le Sueur, Comput. Phys. Commun. **241**, 9 (2019).

[35] D. E. Manolopoulos, J. Chem. Phys. **85**, 6425 (1986).

[36] M. H. Alexander and D. E. Manolopoulos, J. Chem. Phys. **86**, 2044 (1987).

[37] J. M. Hutson, New J. Phys. **9**, 152 (2007).

[38] J. M. Hutson, M. Beyene, and M. L. González-Martínez, Phys. Rev. Lett. **103**, 163201 (2009).

[39] M. D. Frye, B. C. Yang, and J. M. Hutson, Ultracold collisions of Cs in excited hyperfine and Zeeman states [dataset], Durham University (2019), http://dx.doi.org/10.15128/r19p290935v